ISSN 1070-3284, Russian Journal of Coordination Chemistry, 2009, Vol. 35, No. 1, pp. 57–64. © Pleiades Publishing, Ltd., 2009.
Original Russian Text © G.A. Kostin, A.O. Borodin, Yu.V. Shubin, N.V. Kurat'eva, V.A. Emelyanov, P.E. Plyusnin, M.R. Gallyamov, 2009, published in Koordinatsionnaya Khimiya, 2009, Vol. 35, No. 1, pp. 57–64.

Heterometallic Complexes of Co^{2+}, Ni^{2+}, and Zn^{2+} with the $[RuNO(NO_2)_4OH]^{2-}$ Anion and Pyridine: Synthesis, Crystal Structure, and Thermolysis

G. A. Kostin[a]*, A. O. Borodin[a], Yu. V. Shubin[a], N. V. Kurat'eva[a], V. A. Emelyanov[a], P. E. Plyusnin[a], and M. R. Gallyamov[b]

[a] *Institute of Inorganic Chemistry, Siberian Division, Russian Academy of Sciences, pr. akademika Lavrent'eva 3, Novosibirsk, 630090 Russia*

[b] *Novosibirsk State University, ul. Pirogova 2, Novosibirsk, 630090 Russia*

* *E-mail: kostin@che.nsk.ru*

Received February 11, 2008

Abstract—Three new heteronuclear complexes $[Ru(NO)(NO_2)_4(OH)M(Py)_3]$ (M = Co^{2+}, Ni^{2+}, Zn^{2+}) were synthesized and structurally characterized. In all compounds, the $[Ru(NO)(NO_2)_4(OH)]$ fragment is coordinated to the M atom by a bridging OH and two bridging NO_2 groups. The coordination environment of the metal also includes three pyridine nitrogen atoms. Thermal decomposition of cobalt and nickel complexes in an inert atmosphere yields bimetallic solid solutions.

DOI: 10.1134/S1070328409010126

Nano-sized metallic and metal oxide systems are of considerable interest owing to their potential use for the design of catalysts, ceramics, powder and film materials. Research along this line resulted in the development of numerous synthetic procedures based on the use of easily decomposing metal complexes or organometallic compounds, i.e., molecular precursors. Precursors containing atoms of two or more metals within the same molecule are most promising for the design of mixed bi- and polymetallic phases. The main advantage of these compounds is their stoichiometricity, which strictly specifies the composition of the resulting phases. Moreover, such precursors can be directly precipitated from solutions onto a substrate, which allows the production of heterometallic particles supported on various porous substrates.

Salts containing a complex cation of one metal and a complex anion of another metal were proposed to produce highly dispersed powders of solid solutions (Ir–Pd, Rh–Pd, Co–Pd, Co–Pt) [1, 2]. An extensive range of alkoxide [3–5] and carboxylate [6] complexes was used to prepare mixed oxide phases $M_1M_2O_x$. Heterometallic complexes with bis(3-hydroxysalicylidene)ethylenediamine were proposed for the production of superconducting ceramics based on lanthanide oxides [7].

For obtaining compounds, precursors of metal alloys, it is desirable to use complexes stable under conditions of syntheses. Nitroso compounds are perhaps the only class of ruthenium derivatives stable against redox transformations. The $[Ru(NO)(NO_2)_4(OH)]^{2-}$ anion is one of ruthenium complexes most stable in aqueous solutions [8] and easily obtained in a nearly yield from commercial ruthenium trichloride [9]. Previously we found that this anion can function as a tridentate ligand with respect to cobalt, nickel, and zinc complexes with triphenylphosphine oxide (TPPO) [10]. The distances between the ruthenium and transition metal atoms in these heteronuclear complexes are relatively short (3.27–3.39 Å), which allows considering these compounds as the most promising precursors for the preparation of bimetallic solid solutions. However, the presence of a phosphoryl group in the described compounds may give rise to undesired products of thermolysis, e.g., phosphates and phosphides. The replacement of TPPO by a phosphorus-free neutral organic ligand would eliminate this problem.

The purpose of this work was to prepare and study the structures and thermal properties of heteronuclear pyridine complexes of Co, Ni, and Zn with the $[Ru(NO)(NO_2)_4(OH)]^{2-}$ anion.

EXPERIMENTAL

All the reagents and solvents used in the work were at least reagent grade. $Na_2[Ru(NO)(NO_2)_4(OH)] \cdot 2H_2O$ was synthesized from ruthenium(III) chloride according to a reported procedure [9]. The IR spectrum and X-ray diffraction pattern of the obtained compound were consistent with published data [11, 12]. The complexes $M(Py)_4(NO_3)_2 \cdot 2Py$ ("$M(Py)_6(NO_3)_2$") prepared by a previously described procedure [13] were used immediately after preparation.

The UV/Vis spectra of solutions of the complexes in acetone were measured on a Shimadzu UV1700 spec-

trophotometer and the IR spectra were recorded on a Specord M80 instrument (KBr pellets).

Powder X-ray diffraction analysis of the complexes was carried on a DRON-SEIFERT-RM4 diffractometer (CuK_α radiation, graphite monochromator on a reflected beam). The X-ray diffraction patterns were recorded in a step-by-step mode in the 2θ range of 5°–60° for the complex salts and in the 5°–135° range for the thermolysis products. The phase compositions of solid solutions were estimated proceeding from the additivity of atomic volumes.

Thermal analysis was carried out on a Q-1000 Paulik–Paulik–Erdey derivatograph in a helium atmosphere in open crucibles at a heating rate of 10 K/min.

Synthesis of $[Ru(NO)(NO_2)_4(OH)M(Py)_3]$ (M = Ni (I), Co (II), or Zn (III)). Exact weighed portions of $M(Py)_6(NO_3)_2$ (0.1 mmol) and $Na_2[RuNO(NO_2)_4OH] \cdot 2H_2O$ (0.1 mmol) were dissolved in a minimum volume of acetone or ethanol (3–5 ml). After stirring for 1 to 2 h, the solution was concentrated to 2 ml and the precipitated $NaNO_3$ was separated. An excess of hexane (10–15 ml) was added to the filtrate to precipitate heterometallic complexes **I–III** as finely crystalline powders (red for complex **II** and light yellow for complexes **I** and **III**). Yield 88–95%.

For $C_{15}H_{16}N_8O_{10}RuNi$ (I)			
anal. calcd. %:	C, 28.7;	H, 2.57;	N, 17.8.
Found (%):	C, 27.8;	H, 2.29;	N, 16.9.

IR (ν, cm^{-1}): 3447 ν(OH); 1907 ν(NO); 1469, 1448, 1419 $\nu_{as}(NO_2)$; 1336, 1311, 1292 $\nu_s(NO_2)$; 840, 829 $\delta(NO_2)$. UV/Vis: 623 nm (ε = 16).

For $C_{15}H_{16}N_8O_{10}RuCo$ (II)			
anal. calcd. %:	C, 28.7;	H, 2.57;	N, 17.8.
Found (%):	C, 27.7;	H, 2.51;	N, 17.3.

IR (ν, cm^{-1}): 3456 ν(OH); 1917 ν(NO); 1462, 1444, 1412 $\nu_{as}(NO_2)$; 1334, 1317, 1292 $\nu_s(NO_2)$; 835, 821 $\delta(NO_2)$. UV/Vis: 519 nm (ε = 81.6).

For $C_{15}H_{16}N_8O_{10}RuZn$ (III)			
anal. calcd. %:	C, 28.4;	H, 2.54;	N, 17.7.
Found (%):	C, 28.1;	H, 2.52;	N, 17.3.

IR (ν, cm^{-1}): 3481 ν(OH); 1909 ν(NO); 1462, 1415 $\nu_{as}(NO_2)$; 1329, 1311, 1300 $\nu_s(NO_2)$; 833, 819 $\delta(NO_2)$.

X-Ray Diffraction. The single crystals of complexes **I–III** were prepared by slow diffusion of hexane into solutions of the complexes in acetone. X-Ray diffraction data (293 K) were collected on a Bruker Nonius X8Apex CCD diffractometer (MoK_α radiation, graphite monochromator, φ,ω-scan mode). The absorption corrections were applied by the SADABS program [14]. The structures of **I–III** were solved by the direct method and refined by full-matrix least squares method (SHELXTL [14]). The position of the hydroxy group hydrogen atom H(9) was determined from the difference electron density synthesis and refined isotropically. The positions of other hydrogen atoms were calculated geometrically. The crystal data and X-ray experiment details for **I–III** are summarized in Table 1 and selected bond lengths and angles are in Tables 2 and 3. The powder X-ray diffraction patterns for **I–III** coincide with theoretical ones calculated for the single crystals.

The CIF files containing full information about the structures of **I–III** are deposited with the Cambridge Crystallographic Data Collection (no. 656431–656433).

RESULTS AND DISCUSSION

The structural units of crystals **I–III** are isostructural $[Ru(NO)(NO_2)_4(OH)M(Py)_3]$ molecules (Fig. 1). The shortest intermolecular distances O(1H)···O(142) $(1-x, 1-y, 1-z)$ vary from 3.032 Å (**II**) to 3.110 Å (**I**). The M atom in complexes **I–III** is coordinated by three nitrogen atoms of the pyridine molecules (Fig. 1), the μ-bridging OH group, and two bidentate bridging nitro groups. The sequence of variation of the bond lengths in the MO_3N_3 polyhedron (M–OH < M–N < M–ONO) is the same for all three compounds. The M–OH distances vary insignificantly from 2.024(3) Å in **II** to 2.063(2) Å in **III**. The average M–N bond lengths are 0.06–0.1 Å greater than M–OH lengths and increase in the sequence 2.090 (**I**) < 2.120 (**III**) < 2.131 Å (**II**). The average M–ONO bond lengths also increase in the sequence 2.131 (**I**) < 2.183 (**II**) < 2.298 Å(**III**). The longest M–ONO distance in complex **III** accounts for the tetrahedral distortion of the ZnO_3N_3 polyhedron, which is also accompanied by an increase in the NMN angles. The Ru–M distances between the metal atoms vary in the same sequence as the M–OMO bond lengths: **I** (Ni) (3.280(1) Å) < **II** (Co) (3.310(3) Å) < **III** (Zn) (3.376(4) Å).

The geometry of the octahedral fragment $[Ru(NO)(NO_2)_4(OH)]$ changes little upon coordination to the metal. The average Ru–OH and Ru–N bond lengths in **I–III** are similar to those in the $[Ru(NO)(NO_2)_4(OH)]^{2-}$ salts with various cations [15, 16]. The most pronounced differences were found in the geometry of terminal (t) and bridging (b) nitro groups. The $(N–O)_b$ distances are systematically greater than $(N–O)_t$; the N(12)–O(122) and N(11)–O(112) bonds with metal-coordinated oxygen atoms are the longest. The coordination of the $[Ru(NO)(NO_2)_4(OH)]^{2-}$ complex anion to the M atom results in a distortion of the RuN_5O octahedron. The ruthenium atom in complexes **I–III** deviates from the $[N_4]$ plane formed by the nitrogen atoms of nitro groups by 0.076–0.083 Å toward the nitroso group. The greatest deviation of the angles at the central atom from the

Table 1. Crystal data, X-ray experiment details, and structure refinement parameters for **I–III**

Parameters	Value		
	I (Ni)	II (Co)	III (Zn)
M	628.14	628.36	634.8
Space group	$P2_1/c$	$P2_1/c$	$P2_1/c$
a, Å	11.4826(4)	11.4581(4)	11.4555(2)
b, Å	19.6933(6)	19.8011(6)	19.7651(4)
c, Å	11.4817(3)	11.4785(3)	11.5060(3)
β, deg	119.742(1)	119.476(1)	119.4980(10)
V, Å^3	2254.34(12)	2267.18(12)	2267.47(8)
Z	4	4	4
F(000)	1256	1252	1264
μ_{Mo}, mm^{-1}	1.575	1.467	1.793
Crystal size, mm	0.32 × 0.26 × 0.16	0.30 × 0.20 × 0.15	0.2 × 0.05 × 0.05
$2\theta_{max}$, deg	25.68	30.89	25.68
Range of reflection indices	$-9 \le h \le 14$ $-24 \le k \le 24$ $-14 \le l \le 13$	$-16 \le h \le 16$ $-24 \le k \le 28$ $-12 \le l \le 16$	$-13 \le h \le 13$ $-24 \le k \le 23$ $-9 \le l \le 14$
The number of reflections	15256	20986	15491
The number of independent reflections R_{int}	4254, 0.0198	7062, 0.0298	4285, 0.0206
The number of reflections with $I \ge 2\sigma(I)$	3765	5155	3690
The number of refined parameters	320	320	320
R ($I > 2\sigma(I)$)	R = 0.0286 wR = 0.0741	R = 0.0444 wR = 0.1340	R = 0.0269 wR = 0.0781
R (all reflections)	R = 0.0341 wR = 0.0767	R = 0.0682 wR = 0.1470	R = 0.0362 wR = 0.0890
GOOF on F^2	1.072	0.973	1.140
Residual electron densit (min/max), e Å^{-3}	–0.592/0.631	–0.762/1.136	–0.726/0.865

Table 2. Geometric parameters (bond length, Å, and angle, deg) in the MO_3N_3 polyhedra (M = Ni, Co, Zn) of heterometallic complexes **I–III**

Complex		d(M–OH)	d(M–N)	d(M–ONO)	NMN angle	Ru···M, Å
I		2.027(2)	2.079(2)–2.102(4)	2.116(3); 2.143(2)	93.9(1)–98.7(1)	
	average		2.090	2.130	95.6	3.280(1)
II		2.024(3)	2.111(3)–2.142(4)	2.174(3); 2.195(3)	92.76(13)–98.88(15)	
	average		2.131	2.185	95.0	3.310(3)
III		2.036(2)	2.113(4)–2.126(3)	2.279(2); 2.316(2)	95.5(1)–103.8(1)	
	average		2.120	2.298	98.4	3.376(4)

theoretical value of 90° (6.1°–6.9°) was noted for the O(1H)RuN(11) angles. The invariable orientation of the OH group in the heterometallic complexes **I–III** results in the formation of an intramolecular hydrogen bond, O(1H)–H(9)···O(132). The O(1H)···O(132) distance increases slightly in the sequence **I < II < III** and lies in the range of 2.283(3)–2.837(4) Å.

It is of interest that the nature of the organic ligand (TPPO or pyridine) affects only slightly the basic features of the M/Ru coordination unit. A comparison of complex **I** and its triphenylphosphine oxide analog (**IV**) [10] (Fig. 2) showed the most pronounced difference between atom coordinates for the oxygen atoms of terminal nitro groups (0.2–0.7 Å). It is evident that these deviations, as well as the large thermal ellipsoids for these atoms, are mainly due to rotational vibrations along the Ru–N bond. The differences between the positions of metal atoms (Ru and M), bridging atoms

Table 3. Bond lengths (*d*, Å) and bond angles (deg) in the $[RuNO(NO_2)_4OH]$ fragments of heterometallic complexes **I–III**

Complex	*d*(Ru–NO)	*d*(Ru–OH)	$NO_{2(t)}$*			$NO_{2(b)}$*			
			d(Ru–NO_2)	*d*(N–O)	ONO angle	*d*(Ru–NO_2)	*d*(N–O) (O(111), O(121))	*d*(N–O) (O(112), O(122))	ONO angle
I	1.764(3)	1.954(2)	2.079(4)	1.21(5)	119.0(9)	2.093(2)	1.220(3)	1.264(3)	118.4(2)
II	1.759(3)	1.964(2)	2.077(3)	1.21(4)	118(2)	2.094(5)	1.218(4)	1.258(1)	118.4(5)
III	1.759(2)	1.956(3)	2.079(5)	1.21(3)	118.4(11)	2.090(5)	1.224(6)	1.252(2)	118.8(3)

* For the terminal and bridging NO_2 groups, the average distances and angles are given. The errors of their determination are represented as root-mean-square deviations.

(O(1H), N(11), O(112), N(12), O(122)), and rigidly coordinated nitroso group in structures **I** and **IV** do not exceed 0.1 Å. A comparison of the geometry of RuN_5O polyhedra shows that on passing from TPPO to pyridine complexes, the Ru–NO and Ru–OH distances increase by 0.005–0.026 Å for all metals (Co, Ni, Zn). The most pronounced change in these bond lengths is noted for Ni complexes (0.012 Å for Ru–OH and 0.026 Å for Ru–NO). The variation of the Ru–NO bond lengths is antiparallel to the variation of *d*(N≡O): this bond in the nitroso group is on average 0.01 Å shorter for complexes **I–III** than for the phosphine oxide analogs. The Ru–NO_2 bond is less dependent on the ligand nature: the difference between the pyridine and phosphine oxide complexes does not exceed 0.007 Å (Ru–$NO_{2(t)}$) and 0.004 Å (Ru–$NO_{2(b)}$).

The IR spectra of pyridine complexes **I–III** are qualitatively the same as the spectra of TPPO analogs [10]. The stretching region of nitro groups exhibits three bands $\nu_s(NO_2)$ and $\nu_{as}(NO_2)$. For complex **III**, the bands for bridging NO_2 groups (ν_{as} – 1462, ν_s 1300 cm^{-1}) are manifested only as shoulders on stronger bands (1448 and 1311 cm^{-1}). On passing to **I** and **II**, the intensity of vibration bands at 1460 and 1300 cm^{-1} increases, which is in line with shortening of M–ONO_2 bands and, hence, with enhancement of the M–ONO_2 interaction in the sequence Zn < Co < Ni. The presence of two types of NO_2 groups ($NO_{2(t)}$ and $NO_{2(b)}$) in complexes **I–III** is

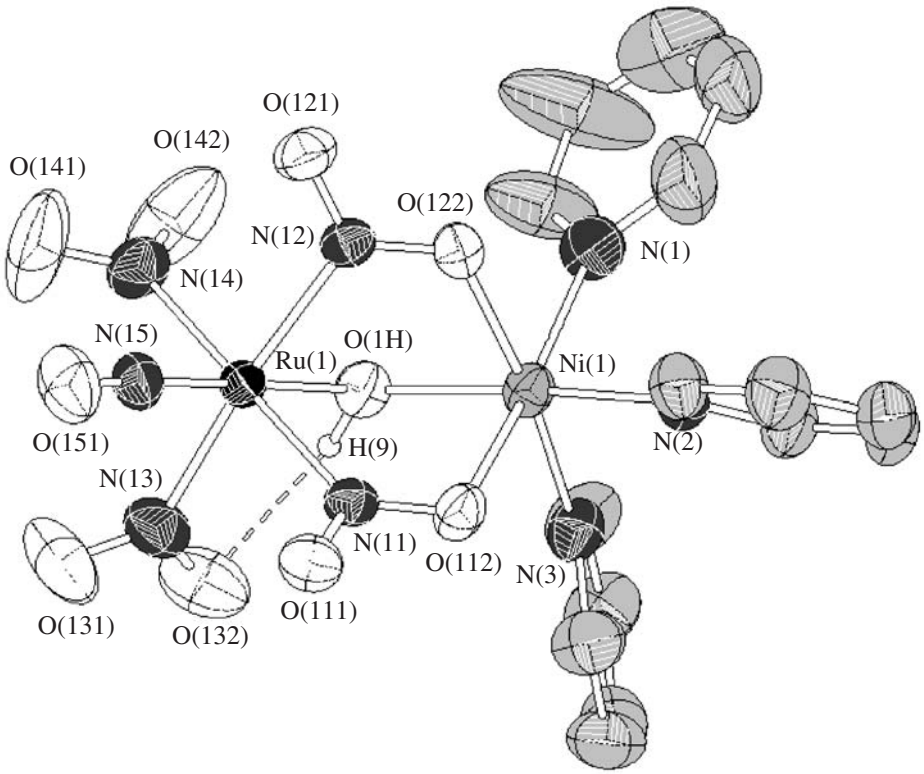

Fig. 1. Structure of molecule **I** (the thermal ellipsoids are given with 50% probability; the hydrogen atoms except for H(9) are omitted).

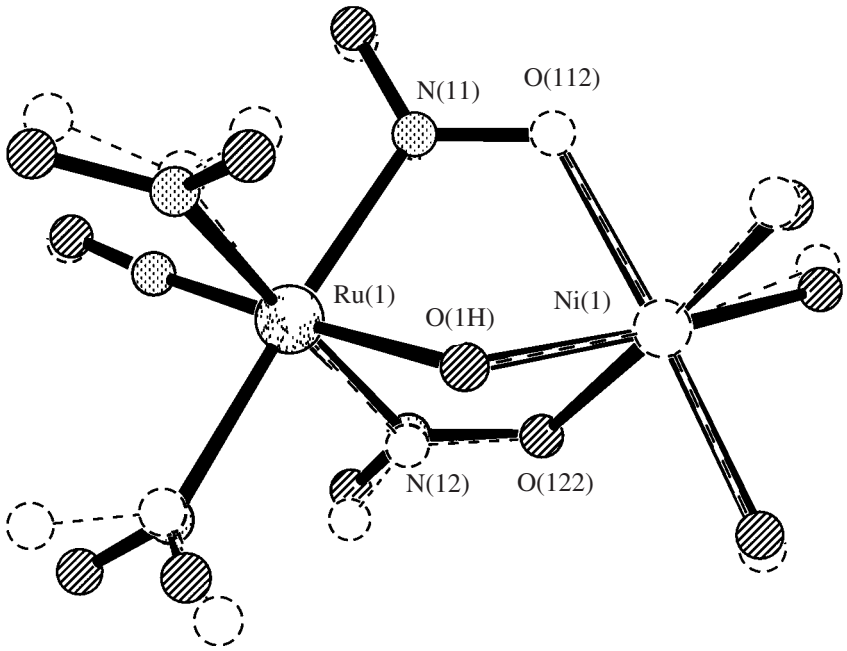

Fig. 2. Comparison of the coordination environments of Ni and Ru atoms in $[RuNO(NO_2)_4OHNi(Ph_3PO)_3]$ (continuous lines) and $[Ru(NO)(NO_2)_4(OH)Ni(Py)_3]$ (**I**) (dashed lines).

also confirmed by the presence of two absorption bands in the $\delta(NO_2)$ bending region. As for TPPO complexes, the absorption maximum of the broad ν(OH) band (3447–3481 cm^{-1}) is shifted to lower frequencies with respect to the spectrum of the $[Ru(NO)(NO_2)_4(OH)]^{2-}$ complex anion. As noted above, transition from TPPO complexes to pyridine complexes **I–III** results in a decrease in *d*(N≡O) by on average 0.01 Å, which is accompanied by a short-wavelength shift (Δ = 10–20 cm^{-1}) of the ν(NO) absorption band in the IR spectra.

In the UV/Vis spectra of solutions of **I** and **II**, the *d–d* transition band for M^{2+} shifts to shorter wavelengths with respect to that of phosphine oxide complexes. This shift is expectable, as field splitting parameters are greater for N-donor ligands than for O-donor ligands [17]. The molar extinction coefficients (**ε**) for pyridine and phosphine oxide complexes are similar and the increase in ε on going from **I** to **II** is related to a pronounced distortion of the CoN_3O_3 polyhedron in solution.

Table 4. Results of thermal decomposition of heterometallic complexes **I–III** and similar complexes with TPPO (An = $[Ru(NO)(NO_2)_4(OH)]$)

Complex	Atmosphere	T_{start}	T_{fin}	Final mass, %	Decomposition products
I	He	143	480	36.8	$Ni_{0.25}Ru_{0.75} + Ni_{0.95}Ru_{0.05}$
II	He	151	515	30.8	$Co_{0.5}Ru_{0.5}$
III	He	115	410	35	ZnO + Ru
$[Ni(TPPO)_3An]$	He	209	560	41.5	*
	Air	261	540	48.8	*
$[Co(TPPO)_3An]$	He	195	585	39.4	*
	Air	265	540	46.1	$Ru + Co_2P_4O_{12}$
$[Zn(TPPO)_3An]$	He	192	590	42.8	*
	Air	274	560	46.1	*

* The decomposition products are amorphous to X-rays.

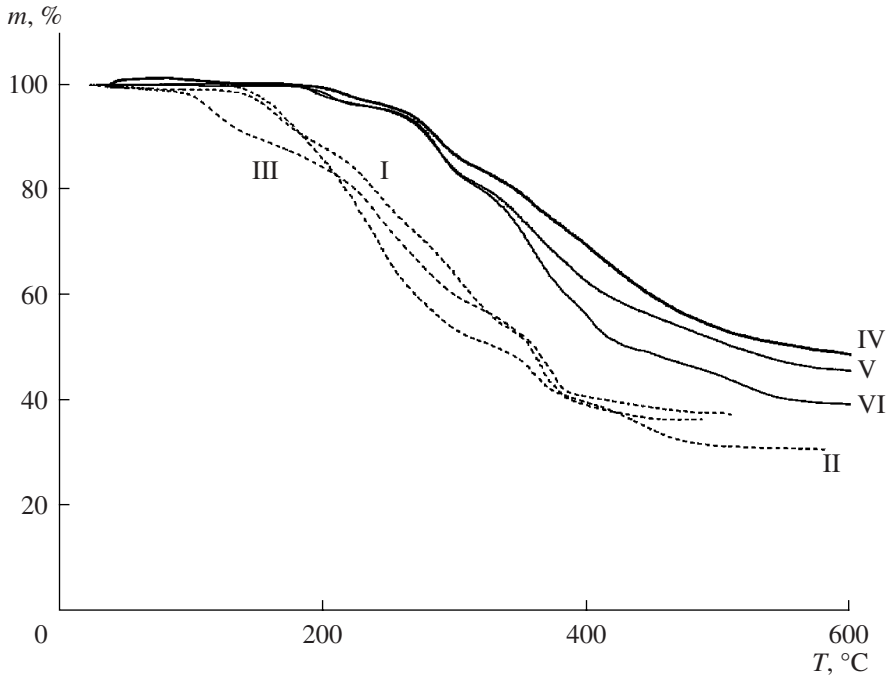

Fig. 3. Thermograms of complexes **I**–**VI**.

The TGA curves for **I**–**III** and for analogous heteronuclear complexes with TPPO prepared by a reported procedure [10] are shown in Fig. 3. The compounds decompose in two or three stages, the temperature of the onset of decomposition for pyridine complexes **I**–**III** being 90–100°C lower than for TPPO analogs (Table 4). Previously [18, 19], it was shown that the first stage of thermal decomposition of different $[Ru(NO)(NO_2)_4(OH)]^{2-}$ salts is associated with elimination of the OH group. The weight loss of mass corresponding to this stage (40–50 a.m.u) implies the removal of at least one nitro group with the hydroxy group. In the TPPO heterometallic complexes, the first endothermic stage occurs at 200–220°C with loss of ~50–60 a.m.u., which coincides with the pattern of decomposition of the ruthenium anion. In pyridine complexes **I**–**III**, the first decomposition stage (starting at 120–150°C) overlaps with the subsequent stages. In the 250–600°C range, the differential curves of weight loss show two overlapping stages related apparently to the elimination of organic ligands and their oxidation by NO and NO_2 groups.

The products of thermolysis of **I**–**III** after 600°C were identified by powder X-ray diffraction. The only decomposition products noted in the X-ray diffraction patterns are bimetallic mixtures or metal oxides. Since the theoretical loss of mass corresponding to the M–Ru products is lower than the experimental one, we suggest that the final products contain also amorphous carbon formed upon partial oxidation of the ligands.

The Co–Ru system forms a continuous series of solid solutions. The X-ray diffraction pattern of a metal powder obtained by thermolysis of **II** exhibits peaks for the solid solution $Ru_{0.5}Co_{0.5}$ corresponding to the stoichiometry of the starting complex and the positions of peaks correspond to the reference peaks for the solid solution $Ru_{0.50}Co_{0.50}$ ([20], Fig. 4a). It is notable that the obtained sample is highly dispersed, the average crystallite size determined from peak broadening being 40 to 60 Å. The Ni–Ru phase diagram is peritectic. At temperatures below the peritectic point (1550°C), two types of solid solutions are stable [21]: those based on fcc and hcp crystal lattices of nickel and ruthenium, respectively. In the range of 500–700°C, the mutual solubility of these metals is 5–10%. The solid residue obtained after thermal decomposition of **I** is a mixture of two solid solutions based on nickel and ruthenium (Fig. 4b). The composition of these solid solutions was determined using the experimental dependence of the atomic volume ($V_{at} = V/z$) on the composition: $Ni_{0.95}Ru_{0.05}$ (a = 3.540 Å, V_{at} = 11.09 Å^3); $Ni_{0.25}Ru_{0.75}$ (a = 2.661, c = 4.245 Å, V_{at} = 12.99 Å^3) (Table 4). The only products of thermolysis of **III** are ZnO and Ru, despite the fact that qualitative studies demonstrated stability of zinc alloys with platinum metals against oxidation [22, 23]. Most likely, decomposition of **III** results in the formation of separate metal (ruthenium and zinc) phases, which is consistent with the lack of mutual solubility in the Zn–Ru system, the appearance of zinc oxide among the products being due to fast oxidation of finely dispersed zinc in air.

The products obtained upon thermolysis of TPPO complexes are mainly amorphous to X-rays. In all three cases (M = Ni, Co, Zn), the weights of the final prod-

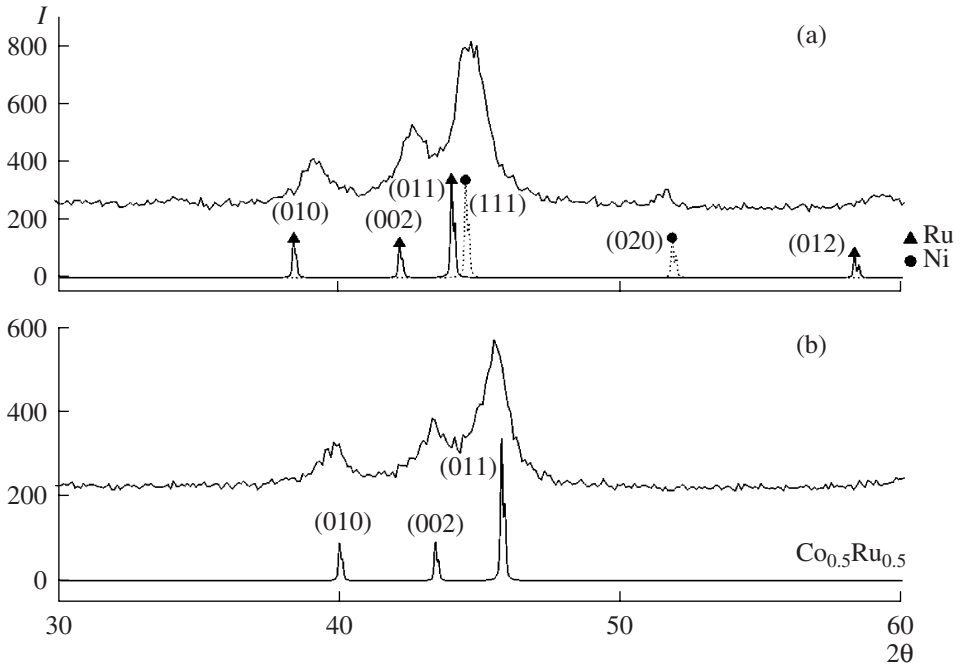

Fig. 4. Experimental X-ray diffraction patterns of the thermolysis products of (a) **I** and (b) **II** and theoretical X-ray diffraction patterns of (a) Ni, Ru powders and (b) the solid solution $Co_{0.5}Ru_{0.5}$.

ucts formed from $[Ru(NO)(NO_2)_4(OH)M(Ph_3PO)_3]$ are higher upon decomposition in air than in an inert (He) atmosphere. This may be due to the fact that phosphorus remains in the thermolysis products as phosphides (in a He atmosphere) or as phosphates (in an oxygen-containing atmosphere). The identified products of $[Ru(NO)(NO_2)_4(OH)Co(Ph_3PO)_3]$ decomposition in air ($Co_2P_4O_{12}$ [20] and ruthenium) indirectly confirm this hypothesis.

Thus, new heterometallic complexes of the nitroso ruthenium anion with transition metals (Co, Ni, Zn) and pyridine were prepared. It was shown that the nature of the organic ligand affects little the structural features of the Ru/M coordination unit; in both TPPO and pyridine complexes, the $Ru(NO)(NO_2)_4(OH)$ fragment is coordinated to the transition metal through bridging hydroxy group and two nitro groups. Thermolysis of pyridine complexes **I**–**III** in an inert atmosphere yields bimetallic solid solutions in the case of cobalt and nickel, while in the case of zinc, two separate metal phases are formed, which is consistent with published data. The samples of solid solutions $Co_{0.5}Ru_{0.5}$ obtained upon annealing of **II** are highly dispersed; the crystallite size is about 40–60 Å.

REFERENCES

1. Korenev, S.V., Venediktov, A.B., Shubin, Yu.V., et al., *Zh. Strukt. Khim.,* 2003, vol. 44, p. 46.
2. Yusenko, K.V., Shubin, Yu.V., Skryabina, O.N., et al., *Zh. Neorg. Khim.*, 2006, vol. 51, no. 4, p. 521 [*Russ. J. Inorg. Chem.* (Engl. Transl.), vol. 51, p. 521].
3. Kessler, V., *Chem. Commun.*, 2003, p. 1213.
4. Purdy, A. and George, C., *Polyhedron*, 1995, vol. 14, p. 761.
5. Boulmaaz, S., Papiernik, R., Hubert-Pfalzgraf, L., et al., *Mater. Chem.,* 1997, vol. 7, p. 2053.
6. Wullens, H., Bodart, N., and Devillers, M., *Solid State Chem.*, 2002, vol. 167, p. 494.
7. Aono, H., Kondo, N., Sakamoto, M., et al., *J. Eur. Ceram. Soc.*, 2003, vol. 23, p. 1375.
8. Fletcher, J.M., Jenkins, I.L., and Lever, F.M., *J. Inorg. Nucl. Chem.*, 1955, vol. 1, p. 378.
9. Zvyagintsev, O.E., Sinitsyn, N.M., and Pichkov, V.N., *Radiokhimiya*, 1964, vol. 6, p. 619.
10. Kostin, G., Borodin, A., Emel'yanov, V., et al., *Mol. Struct.*, 2007, vol. 837, p. 63.
11. Mercer, E.E., McAllister, W.A., and Durig, J.R., *Inorg. Chem.*, 1966, vol. 5, p. 1881.
12. Blake, A.J., Gould, R.O., Johnson, B.F.J., and Parisini, E., *Acta Crystallogr., Sect. C: Cryst. Struct. Commun.*, 1992, vol. 48, p. 982.
13. Soldatov, D.V. and Lipkovski, Ya., *Zh. Strukt. Khim.*, 1995, vol. 36, p. 1070.
14. *APEX2 (Version 1.08), SAINT (Version 7.03), SADABS (Version 2.11) and SHELXTL (Version 6.12). Bruker Advanced X-Ray Solutions*, Madison (WI, USA): Bruker AXS Inc., 2004.
15. Emel'yanov, V.A., Baidina, I.A., Gromilov, S.V., and Virovets, A.V., *Zh. Strukt. Khim.*, 2006, vol. 47, p. 69.

16. Emel'yanov, V.A., Gromilov, S.V., and Baidina, I.A., *Zh. Strukt. Khim.*, 2004, vol. 45, p. 923.
17. Gray, H.B., *Electrons and Chemical Bonding*, New York: Benjamin, 1965.
18. Pichkov, V.N., Zvyagintsev, O.E., and Sinitsyn, N.M., *Zh. Neorg. Khim.*, 1966, vol. 11, p. 2560.
19. Sinitsyn, N.M. and Kokunova, V.N., *Zh. Neorg. Khim.*, 1990, vol. 35, p. 3120.
20. ICDD/JCPDS PDF Database. The International Centre for Diffraction Data Powder Diffraction File, 2001.
21. *Binary Alloy Phase Diagrams*, Massalski, T.B., Ed., Ohio: ASM International, 1996.
22. Zadesenets, A.V., Filatov, E.Yu., Yusenko, K.V., et al., *Inorg. Chim. Acta*, 2008, vol. 361, no. 1, p. 199.
23. Kozitsyna, N.Yu., Vargaftik, M.N., Nefedov, S.E., and Moiseev, I.I., Abstracts of Papers, *XVIII Mezhdunar. Chernyaevskaya konf. po khimii, analizu i tekhnologii platinovykh metallov* (XVIII Intern. Chernyaev Conf. on the Chemistry, Analysis and Technology of Platinum Metals), Part 1., Moscow, 2006, p. 14.